

## AS ANATOMICAL FEATURES OF THE XYLEM COULD INFLUENCE WOUND HEALING PROCESS IN TREES?<sup>1</sup>

## COMO AS CARACTERÍSTICAS ANATÔMICAS DO XILEMA PODEM INFLUENCIAR NO PROCESSO DE CURA DE FERIMENTOS EM ÁRVORES?<sup>1</sup>

Diego ROMEIRO <sup>2</sup>; Camila Moura SANTOS <sup>3</sup>; Luís Alberto BUCCI <sup>3</sup>; Eduardo Luiz LONGUI <sup>3,4</sup>

**ABSTRACT** - Since trees are continually at risk of damage from animals and adverse environmental conditions, their survival depends on wound healing capacity. Common physiological responses to injury are cell proliferation, regeneration of the vascular tissue and the formation of compounds to protect cells near the wound. The wood anatomy is important for understanding the mechanisms of wound healing, and hence tree survival. We studied twelve tropical tree species to understand how some wood characteristics contribute to the wound healing process. We made the quantitative analysis of wood characteristics and evaluated the rate of wound healing two years after the collection of samples. Species with a large amount of axial parenchyma, presented the highest wound healing rate, proving that axial parenchyma cell supply material for greater cell proliferation, acting to close the wound much faster. Species that have axial parenchyma and produce a network between vessels and rays through living tissue, recover and provide passage of hormones that stimulate cell division of tissue near the wound, promoting growth of callus tissue all around the wound area, accelerating wound closure. On the other hand, the absence of axial parenchyma hinders such recovery by disabling affected regions; both above and below the injury, from producing sufficient wound healing tissue. The presence of longer fibers is an indicative of a larger amount of gibberellin that is involved in cell division during wound healing; therefore, species with longer fibers had faster wound healing.

Keywords: Axial parenchyma; Fibers, Translocation; Tropical trees; Wood anatomy.

**RESUMO** - As árvores estão continuamente em risco de danos por animais e condições ambientais adversas, sua sobrevivência depende da capacidade de cicatrização de feridas. Respostas fisiológicas comuns à lesão são a proliferação celular, regeneração do tecido vascular e formação de compostos para proteger as células próximas à ferida. Conhecer a anatomia da madeira é essencial para compreender os mecanismos de cicatrização de feridas e sobrevivência da árvore. Estudamos 12 espécies tropicais para entender como algumas características da madeira contribuem para o processo de cicatrização de feridas. Fizemos a análise quantitativa das características da madeira e avaliamos a taxa de cicatrização das feridas dois anos após a coleta das amostras. Espécies com grande quantidade de parênquima axial, apresentaram maior taxa de cicatrização da ferida, comprovando que células do parênquima axial fornecem material para maior proliferação celular, agindo mais rápido no fechamento da ferida. Espécies com parênquima axial arranjado de forma a produzir uma rede entre vasos e raios através do tecido vivo, se recuperam e fornecem a passagem de hormônios que estimulam a divisão celular do tecido próximo à ferida, promovendo o crescimento de tecido em toda a área da ferida, acelerando seu fechamento. A ausência de parênquima axial dificulta essa recuperação por incapacitar as regiões afetadas; acima e abaixo da lesão, de produzir tecido suficiente para cicatrização de feridas. A presença de fibras mais longas é indicativo de maior teor de giberelina, envolvida na divisão celular durante a cicatrização; portanto, espécies com fibras mais longas tiveram cicatrização mais rápida das feridas.

Palavras-chave: Parênquima axial; Fibras; Translocação; Árvores tropicais; Anatomia da madeira.

<sup>1</sup> Recebido para análise em 19.02.2021. Aceito para publicação em 09.06.2021.

<sup>2</sup> Instituto de Pesquisas Ambientais, Av. Miguel Estéfano 3687, 04301-902, Água Funda, São Paulo, SP, Brazil,

<sup>3</sup> Instituto de Pesquisas Ambientais, Rua do Horto 931, -02377-000, Horto Florestal, São Paulo, SP, Brazil.

<sup>4</sup> Autor para correspondência: Eduardo Luiz Longui – edulongui@gmail.com

## 1 INTRODUCTION

Plants routinely exposed to adverse environmental factors can be easily wounded. Thus, mechanical processes that destroy cells and tissues may expose inner parts of the plant (Imaseki, 1985). Physiological responses to such injuries vary, however, the fundamental result is the regeneration of the affected tissue. Thus, the production of compounds to protect cells near the wound, cell proliferation, and regeneration of vascular tissues are common responses (Imaseki, 1985) closely related to wood anatomy (Aloni, 2007, 2010).

Stem anatomy has been largely studied for functional traits related to mechanical support, as well as storage and hydraulic conductivity linked to life history traits. Many studies have reported that drought-induced forest decline is a result of failure in water transport system in a large number of woody species (Choat et al., 2012). To recover hydraulic function interrupted by cavitation, the parenchyma cells play an important role by secreting solutes into the vessels that establish an osmotic gradient and thereby promote their recovery (Tyree et al., 1999; Zwieniecki and Holbrook, 2009; Brodersen et al., 2010). Parenchyma cells are also involved in the storage of water, sugar and mineral nutrients, regulation of transpiration (Borchert and Pockman, 2005) and others processes such as leaf-flushing (Chapotin et al., 2006). These features help woody species to avoid drought stress. Parenchymatous tissue promotes decay resistance by producing extractives (Schwarze, 2007) and avoiding the spread of pathogens once it is involved in formation of tyloses inside the vessels (Yadeta and Thomma, 2013).

These features are linked to tree's life history and are predictors of tree longevity. In forest ecology, the main causes of death in trees are exogenous disturbances and senescence (Toledo et al., 2013), associated with weather stress (Ostry et al., 2011). Many such exogenous disturbances result in wounds and large or deep wounds cause direct damage by inhibiting or altering the xylem and phloem transport (Neely, 1988), besides it also facilitates the invasion of opportunistic or pathogenic organisms (Neely, 1988; Ostry et al., 2011). Therefore, the objective of this study is to understand how remaining anatomical characteristics of xylem could influence the wound healing process, to reduce the healing time or distribution of callus production.

## 2 MATERIALS AND METHODS

### 2.1 Sample selection

Five trees with more than 10 cm in trunk diameter were chosen for each of the twelve species studied. Samples from each tree were collected at breast height (DBH, 1.3 m from the ground) with a non-destructive technique using a bow saw, hammer and chisel. Samples were collected for analysis producing a wound with approximately 4 cm high, 12 cm wide and 1.5 cm deep. Samples of *Alchornea glandulosa* Poepp. & Endl., *Paubrasilia echinata* Lam., *Cariniana legalis* (Mart.) Kuntze, *Cariniana estrellensis* (Raddi) Kuntze, *Ceiba speciosa* (A.St.-Hil.) Ravenna, *Gallesia integrifolia* (Spreng.) Harms, *Guazuma ulmifolia* Lam., *Handroanthus chrysotrichus* (Mart. ex DC.) Mattos, *Handroanthus heptaphyllus* (Vell.) Mattos., *Inga sessilis* (Vell.) Mart., *Maclura tinctoria* (L.) D. Don ex Steud., and *Peltophorum dubium* (Spreng.) Taub. were collected in the arboretum located at the Alberto Löfgren State Park, São Paulo, SP, Brazil (23°27'S – 46°38'W, elevation 814m, Figure 1). The number registration in the Forestry Institute Xylarium (SPSFw) and number of the individual in the arboretum were shown in Table 1, and forestry characteristics were measured and shown in Table 2.

Table 1. Species studied with the respective registration number in the Forestry Institute Xylarium (SPSFw) and number of the individual in the arboretum.

Tabela 1. Espécies estudadas com o respectivo número de registro na Xiloteca do Instituto Florestal (SPSFw) e número do indivíduo no plantio.

Species/Family	Nº of SPSFw	Nº arboretum
<i>Alchornea glandulosa</i> Poepp. & Endl. (Euphorbiaceae)	5079	255
	5080	256
	5081	304
	5082	361
	5083	402
<i>Paubrasilia echinata</i> Lam. (Fabaceae- Caesalpinoideae)	5084	194
	5085	217
	5086	297
	5087	368
	5088	455
<i>Cariniana legalis</i> (Mart.) Kuntze (Lecythidaceae)	5089	21
	5090	50
	5091	137
	5092	224
	5093	344
<i>Cariniana estrellensis</i> (Raddi) Kuntze (Lecythidaceae)	5094	175
	5095	240
	5096	269
	5097	436
	5098	449

to be continued  
continua

continuation - Table 1  
 continuação - Tabela 1

<i>Ceiba speciosa</i> (A.St.-Hil.) (Malvaceae)	Ravenna	5099	190
		5100	268
		5101	299
		5102	326
		5103	407
<i>Gallesia integrifolia</i> (Phytolaccaceae)	Harms	5104	107
		5105	198
		5106	265
		5107	315
		5108	442
<i>Guazuma ulmifolia</i> Lam. (Malvaceae)		5109	68
		5110	98
		5111	99
		5112	130
		5113	182
<i>Handroanthus chrysotrichus</i> (Mart. ex DC.) (Bignoniaceae)	Mattos.	5114	225
		5115	253
		5116	305
		5117	325
		5118	390
<i>Handroanthus heptaphyllus</i> (Vell.) Mattos. (Bignoniaceae)		5119	16
		5120	23
		5121	154
		5122	262
		5123	434
<i>Inga sessilis</i> (Vell.) Mart. (Fabaceae-Mimosoideae)		5124	232
		5125	334
		5126	371
		5127	374
		5128	408
<i>Maclura tinctoria</i> (L.) D. Don ex Steud. (Moraceae)		5129	6
		5130	40
		5131	71
		5132	151
		5133	293
<i>Peltophorum dubium</i> (Fabaceae-Caesalpinioideae)	Taub.	5134	128
		5135	252
		5136	369
		5137	379
		5138	450

## 2.2 Anatomical analyses

In order to obtain quantitative data of the woods, cross sections of each sample were made using a sliding microtome. Transverse, tangential and radial longitudinal sections of 15-20µm thickness were stained with 1% aqueous solution of safranin; sections were mounted in glycerin (50 %) and imaged using a digital camera coupled to an Olympus CX31 microscope. Vessel and fiber characteristics were determined after maceration for 8h at 55 to 60 °C following Kraus and Arduin (1997) and staining with ethanolic solution of safranin (1%).

Anatomical measurements followed the IAWA Committee (1989) recommendations. Vessel

diameter, vessel frequency, vessel element length, diameter of intervessel pits and vessel ray pits were measured. We also measured height, width and ray frequency and length, diameter and wall thickness of fibers. Axial parenchyma proportion was determined by subtracting the total area of axial parenchyma from the entire imaged cross-sectional area.



Figure 1. a. Collection area located at Alberto Löfgren State Park - PEAL. b. General view of “Arboretum 500 Years” commemorating the 500th anniversary of the discovery of Brazil.

Figura 1. a. Área de coleta localizada no Parque Estadual Alberto Löfgren - PEAL. b. Vista geral do “Arboreto 500 anos” em comemoração aos 500 anos do descobrimento do Brasil.

## 2.3 Wood density

Wood density was determined on samples from diameter at breast height by the ratio between the oven-dry mass and the green volume of samples (Glass and Zelinka, 2010).

## 2.4 Wound healing

Wound healing progress was monitored for two years and imaged for measurements at the end of this period. The images were measured on Image Pro Plus 6.0 and wound healing area proportion was determined by subtracting the total area without healing tissue from the entire wounded area.

Table 2. Mean forestry characteristics of studied species.

Tabela 2. Características florestais médias das espécies estudadas.

Species	Height (m)	DBH (cm)
<i>Alchornea glandulosa</i>	11.5 (2.9)	34.7 (5.1)
<i>Paubrasilia echinata</i>	11.7 (2.7)	12.7 (2.3)
<i>Cariniana estrellensis</i>	16.7 (3.8)	26.7 (6.5)
<i>Cariniana legalis</i>	15.0 (3.3)	21.6 (2.1)
<i>Ceiba speciosa</i>	13.0 (4.0)	30.1 (5.7)
<i>Gallesia integrifolia</i>	16.2 (5.5)	28.8 (11.4)
<i>Guazuma ulmifolia</i>	17.2 (2.4)	33.4 (4.2)
<i>Handroanthus chrysotrichus</i>	9.5 (2.2)	14.7 (8.6)
<i>Handroanthus heptaphyllus</i>	12.5 (1.4)	17.4 (4.2)
<i>Inga sessilis</i>	14.5 (4.1)	41.1 (6.3)
<i>Maclura tinctoria</i>	16.5 (0.5)	27.3 (5.4)
<i>Peltophorum dubium</i>	17.6 (3.7)	25.8 (8.1)

Standard deviations shown in parentheses. DBH = diameter at breast height (1.3 m from the ground).

Desvios padrão mostrados entre parênteses. DBH = diâmetro à altura do peito (1,3 m do solo).

## 2.5 Statistical analyses

Pearson correlation was used to show relationships between anatomical characteristics, wood density and wound healing proportion. Results with  $p < 0.05$  were considered significant. We use a bidirectional stepwise elimination procedure to determine a final regression model for wound healing and wood characteristics. All variables were standardized before analysis. Statistical analyses were also performed using R 3.1.3 (R Core Team, 2015), package *vegan* (Oksanen et al., 2015), package *Rcmdr* (Fox, 2005) and package *scatterplot3d* (Ligges and Mächler, 2003).

Table 3. Qualitative description of studied species.

Tabela 3. Descrição qualitativa das espécies estudadas.

Species	Qualitative anatomical characteristics
<i>Alchornea glandulosa</i>	Axial parenchyma diffuse-in-aggregates; uniseriate rays; circular, alternate intervessel pits; low distinct growth rings.
<i>Paubrasilia echinata</i>	Axial parenchyma confluent in short sections; multiseriate, storied rays; polygonal, alternate, vested intervessel pit; growth rings boundaries distinct by axial parenchyma line.

to be continued  
continua

continuation - Table 3  
 continuação - Tabela 3

<i>Cariniana estrellensis</i>	Axial parenchyma reticulate, multiseriate rays; alternate circular and / or polygonal intervessel pits; distinct growth rings and bounded by a fibrous zone.
<i>Cariniana legalis</i>	Axial parenchyma reticulate multiseriate rays; alternate polygonal intervessel pits; distinct growth rings and bounded by a fibrous zone.
<i>Ceiba speciosa</i>	Axial parenchyma diffuse-in-aggregates; multiseriate rays; circular, alternate intervessel pits; distinct growth rings and bounded by a fibrous zone.
<i>Gallesia integrifolia</i>	Axial parenchyma diffuse; phloem even alternated by conjunctive parenchyma tissue; multiseriate rays; circular, alternate intervessel pits; structurally, the vascular cylinder is composed by successive rings of secondary xylem and phloem.
<i>Guazuma ulmifolia</i>	Axial parenchyma diffuse and / or diffuse in aggregates; multiseriate rays; circular, alternate intervessel pits; low distinct growth rings, bounded by a fibrous zone.
<i>Handroanthus chrysotrichus</i>	Axial parenchyma aliform confluent in long strands; ray width 1 to 2 cells, storied rays; circular, alternate intervessel pits; distinct growth rings delimited by parenchyma line and fibrous zone.
<i>Handroanthus heptaphyllus</i>	Axial parenchyma aliform confluent; multiseriate, storied rays; circular, alternate and or opposite intervessel pits; distinct growth rings and bounded by a thin line of parenchyma and fibrous zone.
<i>Inga sessilis</i>	Axial parenchyma aliform confluent; ray width 1 to 2 cells; circular, alternate, vestured intervessel pits; distinct growth rings and bounded by a fibrous zone.
<i>Maclura tinctoria</i>	Axial parenchyma aliform with confluent linear extension; multiseriate rays; circular, alternate intervessel pits; distinct growth rings and bounded by a fibrous zone.
<i>Peltophorum dubium</i>	Axial parenchymal lozenge-aliform; ray width 1 to 2 cells; circular, alternate intervessel pits; distinct growth rings and bounded by a parenchyma line.

Use the information in this table to better understand the figures 4-10

Use as informações dessa tabela para melhor entendimento das figuras 4-10

Table 4. Quantitative anatomical features, mean values and (standard deviations).

Tabela 4. Características anatômicas quantitativas, valores médios e (desvios padrão).

Species	PP	VEL	FL	FWT	VD	VF	RH	RW	RF	IP	VRP
<i>Ag</i>	1.59 (0.3)	722.4 (154.0)	1351.0 (183.6)	5.6 (1.0)	214.2 (17.9)	4.6 (0.7)	1059.4 (105.9)	24.2 (1.5)	16.4 (0.9)	13.2 (2.2)	12.9 (1.1)
<i>Pe</i>	3.26 (1.1)	296.7 (46.5)	1068.5 (131.5)	6.2 (0.6)	90.0 (3.3)	19.2 (4.3)	242.5 (25.9)	26.0 (1.8)	9.5 (0.5)	4.5 (0.4)	3.5 (0.4)

to be continued  
 continua

continuation - Table 4  
 continuação - Tabela 4

<i>Ce</i>	7.65 (3.5)	454.1 (89.5)	1627.0 (209.6)	5.4 (0.6)	141.3 (9.0)	10.2 (3.2)	481.5 (32.0)	54.0 (4.9)	8.1 (0.6)	8.1 (0.5)	7.5 (0.5)
<i>Cl</i>	10.15 (2.5)	418.8 (119.8)	1627.2 (207.3)	4.7 (0.2)	90.2 (8.8)	10.7 (1.4)	351.3 (51.4)	38.0 (7.4)	8.1 (0.6)	8.0 (0.4)	6.4 (0.6)
<i>Cs</i>	18.70 (3.2)	390.6 (66.3)	2048.9 (276.0)	6.1 (0.9)	218.2 (18.3)	3.4 (0.8)	922.6 (72.1)	109.1 (34.5)	3.6 (0.4)	14.7 (2.0)	15.2 (0.8)
<i>Gi</i>	9.21 (2.8)	227.9 (52.1)	986.1 (155.7)	4.5 (0.8)	78.6 (22.0)	16.8 (2.1)	699.5 (91.4)	89.2 (91.4)	3.6 (0.3)	10.2 (1.3)	8.0 (1.2)
<i>Gu</i>	3.36 (1.5)	357.2 (50.0)	1440.3 (229.1)	5.6 (0.3)	115.4 (12.9)	12.9 (5.0)	566.9 (59.4)	74.9 (4.6)	6.4 (0.3)	5.1 (0.6)	4.3 (0.3)
<i>Hc</i>	10.62 (1.7)	243.5 (41.0)	1217.5 (143.7)	7.1 (1.4)	83.7 (2.8)	20.7 (3.1)	147.4 (11.0)	42.8 (1.5)	9.3 (0.4)	9.6 (2.5)	5.3 (0.5)
<i>Hh</i>	5.84 (3.4)	219.5 (25.5)	969.4 (161.5)	5.4 (0.5)	66.1 (5.6)	33.7 (5.4)	151.8 (20.0)	35.9 (5.2)	7.6 (0.6)	9.3 (1.4)	5.9 (0.9)
<i>Is</i>	6.78 (3.1)	409.2 (99.8)	1268.8 (184.4)	4.7 (0.5)	184.2 (23.9)	6.3 (2.1)	253.1 (25.5)	32.6 (4.8)	6.8 (0.5)	7.1 (0.6)	6.1 (0.9)
<i>Mt</i>	3.47 (1.5)	278.6 (61.2)	1057.9 (146.8)	4.3 (0.4)	148.4 (16.0)	6.9 (1.5)	272.5 (45.1)	35.5 (4.3)	6.4 (0.5)	7.0 (0.4)	8.0 (0.2)
<i>Pd</i>	5.70 (0.5)	410.0 (116.7)	1297.8 (213.2)	5.3 (0.7)	153.0 (12.5)	4.6 (0.7)	229.5 (26.2)	33.8 (4.9)	9.4 (0.8)	6.5 (0.4)	6.2 (0.7)

PP = parenchyma proportion (% per square millimeter) VEL = vessel element length ( $\mu\text{m}$ ), FL = fiber length ( $\mu\text{m}$ ), FWT = fiber wall thickness ( $\mu\text{m}$ ), VD = vessel diameter ( $\mu\text{m}$ ), VF = vessel frequency (vessels per square millimeter), RH = ray height ( $\mu\text{m}$ ), RW = ray width ( $\mu\text{m}$ ), RF = ray frequency (rays per millimeter), IP = intervessel pit ( $\mu\text{m}$ ), VRP = vessel-ray pit ( $\mu\text{m}$ ). *Ag* = *Alchornea glandulosa*, *Pe* = *Paubrasilia echinate*, *Ce* = *Cariniana estrellensis*, *Cl* = *Cariniana legalis*, *Ce* = *Ceiba speciosa*, *Gi* = *Gallesia integrifolia*, *Gu* = *Guazuma ulmifolia*, *Hc* = *Handroanthus chrysotrichus*, *Hh* = *Handroanthus heptaphyllus*, *Is* = *Inga sessilis*, *Mt* = *Maclura tinctoria* e *Pd* = *Peltophorum dubium*.

PP = proporção de parênquima (% por milímetro quadrado) VEL = comprimento do elemento de vaso ( $\mu\text{m}$ ), FL = comprimento da fibra ( $\mu\text{m}$ ), FWT = espessura da parede da fibra ( $\mu\text{m}$ ), VD = diâmetro de vaso ( $\mu\text{m}$ ), VF = frequência de vaso (vasos por milímetro quadrado), RH = altura do raio ( $\mu\text{m}$ ), RW = largura do raio ( $\mu\text{m}$ ), RF = frequência do raio (raios por milímetro), IP = pontuação intervascular ( $\mu\text{m}$ ), VRP = pontuação raiovascular ( $\mu\text{m}$ ). *Ag* = *Alchornea glandulosa*, *Pe* = *Paubrasilia echinate*, *Ce* = *Cariniana estrellensis*, *Cl* = *Cariniana legalis*, *Ce* = *Ceiba speciosa*, *Gi* = *Gallesia integrifolia*, *Gu* = *Guazuma ulmifolia*, *Hc* = *Handroanthus chrysotrichus*, *Hh* = *Handroanthus heptaphyllus*, *Is* = *Inga sessilis*, *Mt* = *Maclura tinctoria* e *Pd* = *Peltophorum dubium*.

Generally, species with high wood density showed slower wound healing rate, however, some species differ this result as observed in *Inga sessilis* (Figure 2). Species with a large amount of axial parenchyma showed a higher wound healing rate, this result was found in *Cariniana legalis*, *Ceiba speciosa* and *Handroanthus chrysotrichus* (Table 4). On the other hand, *Gallesia integrifolia* and

*Guazuma ulmifolia* also presented a high wound healing rate (Figure 2), but it was promoted by radial parenchyma cells (Table 4), resulting in a positive correlation between ray height, ray width, and wound healing (Table 5). These ratios confirm the importance of axial and radial parenchyma cells on the wound healing process. A negative correlation between ray frequency and wound healing rate was

found, it could be observed principally in *Alchornea glandulosa*, that has more than 10 rays per millimeter (Table 4). A positive relationship was established between fiber length and wound healing (Table 5), as observed in *Ceiba speciosa*, *Cariniana estrellensis* and *C. legalis* (Table 4). After correlation analysis, the tridirectional stepwise showed that parenchyma proportion and fiber length were the main predictors to determine the regression model for wound healing (Figure 3). Using partitioning variation was possible decompose the variation of wound healing model and determine the interaction between predictors.

Two patterns of wound healing were observed: one with formation of callus tissue all around the wound area (Figure 4, a and c) and another only on the sides of the wound (Figure 4, e). Using wood anatomy as a basis for comparison, it was observed that wound healing produces callus tissue around the entire wound when axial parenchyma cells provide a network between vessels and rays (Figure 4 b and d). This was observed most precisely in reticulate parenchyma in *Cariniana estrellensis* and *C. legalis* (Figure 5 a and d), confluent parenchyma in *Handroanthus chrysotrichus* (Figure 8, d) and *Inga sessilis* (Figure 9, d) or in specifically species that the network was produced with vascentric parenchyma, large vessels and rays as observed in *Ceiba speciosa* (Figure 7, a). In contrast, when callus tissue was formed on the sides of wound, as in *Gallesia integrifolia* (Figure 7, d) and *Guazuma ulmifolia* (Figure 9, a), these network between vessels and rays are scarce, once apotracheal parenchyma founded in these two species is not associated with vessels and do not produce connection between vessel and rays.

Likewise, the increased width of vessel pits, as in *Ceiba speciosa*, benefits translocation between cells, thus intensifying cell proliferation which, in turn, results in a positive correlation between wound healing and both intervessel pits and ray vessel pits.

Wood anatomical characteristics are illustrated in figures 5 - 10 and wound healing in figure 11.

#### 4 DISCUSSION

Species with high wood density have a higher construction cost and lower growth rate (Larjavaara and Muller-Landau, 2010). Thus, it is expected that species with high wood density have low rate of wound healing, while species with low wood density have high rate. However, this pattern was not found in all the studied species, as evidenced in *Inga sessilis* and *Peltophorum dubium*. This result shows that wood density is not the sole determinant of wound healing rate. Therefore, we focused on

parenchyma cells because they play an important role in wound healing and regeneration (Evert, 2006).

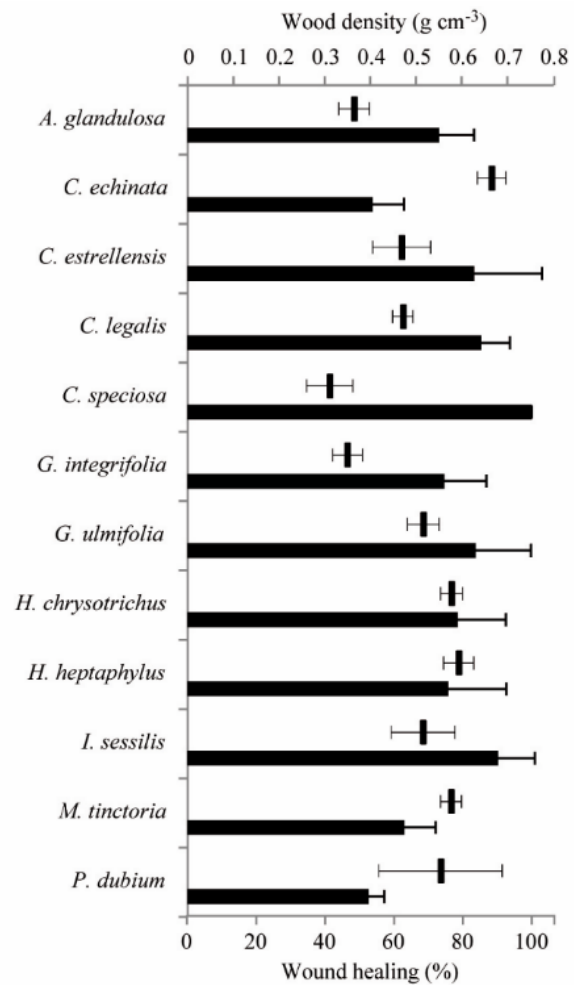


Figure 2. Average of the wound healing and wood density with their respective standard deviations of the studied species.

Figura 2. Média da cicatrização e densidade da madeira com seus respectivos desvios padrão das espécies estudadas.

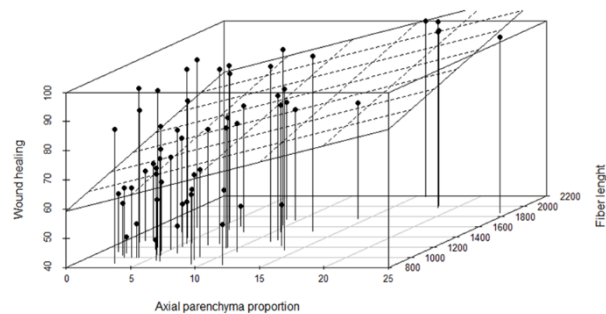


Figure 3. Correlations among wound healing, parenchyma proportion and fiber length.

Figura 3. Correlações entre a cicatrização de feridas, proporção de parênquima e comprimento das fibras.

Table 5. Correlation coefficients between anatomy characteristics with wound healing proportion.

Tabela 5. Coeficientes de correlação entre as características anatômicas com a proporção de cicatrização da ferida.

Anatomy characteristics	Pearson correlation	P
Wood density	- 0.40	0.001
Axial parenchyma proportion	0.48	0.0001
Ray height	0.31	0.01
Ray width	0.42	0.0009
Ray frequency	- 0.30	0.01
Fiber length	0.47	0.0001
Fiber wall thickness	0.01	0.92
Intervessel pit diameter	0.41	0.001
Vessel-ray pit diameter	0.30	0.01
Vessel diameter	0.20	0.12
Vessel density	- 0.12	0.34
Vessel element length	0.11	0.37

The aggregation of axial parenchyma cells represents progressively more efficiency in mobilizing and storing photosynthates and translocating other compounds (Carlquist, 1975). Soluble carbohydrates, such as sucrose and glucose, induce gene expression and seem to interact with hormonal responses (Uggla et al., 2001), benefiting wound healing.

*Ceiba speciosa* with a large amount of axial parenchyma, presented the highest wound healing proportion, proving that axial parenchyma cells supply material for greater cell proliferation, acting to close the wound much faster.

However, Uggla et al. (2001) reported that the presence of carbohydrates is not the sole contributor to this process, but rather the capacity of tissues to use them. The efficiency of photosynthate translocation between axial and radial parenchyma systems depends on their massive contact with xylem vessels and cambial tissue (Carlquist, 1975, 2001). We noted that *Cariniana* species, *Ceiba speciosa*, *Handroanthus* species and *Inga sessilis* presented more that characteristics. Therefore, it can concluded that parenchyma also plays an important role in wound healing, its cellular transdifferentiation capacity promotes transformation of a parenchyma cell into a conduit

which maintain auxin signaling and vascular continuity (Fukuda, 1996; Aloni, 2013).

The amount of axial parenchyma also protects against wood decay through the process of compartmentalization, i.e., the ability to avoid the input of opportunistic pathogens (Arbellay et al., 2012; Morris et al., 2016) that could decrease cellular activity and, correspondingly, decrease the healing process. Hence, trees with good compartmentalization capacity present a faster wound healing rate (Haavik and Stephen, 2011). A large amount of parenchyma benefits tree species by the greater occurrence of parenchyma cells associated with vessels, allowing their obstruction in order to protect healthy tissue. This protection can occur by the formation of tyloses or some compounds (Schmitt and Liese, 1990, 1994) and by suberization in xylem tissues (Imaseki, 1985).

Even though cambial tissue post-injury may have been lost, it is parenchyma tissue that will start the healing process (Neely, 1988). In particular, callus will be formed by parenchyma cells originated from parenchyma tissue remnants or non-differentiated cells. This is the first tissue formed after injury (Stobbe, 2002; Pang et al., 2008). It is parenchyma tissue that has the capacity to regenerate, while other kinds of cells, such as vessels and fibers, have already differentiated and possess secondary walls (Fukuda, 1996). Fisher and Ewers (1989) found a significant relationship between parenchyma tissue and wound healing, i.e., a new xylem parenchyma that stimulates the formation of callus that quickly rejoins the exposed surface.

In this work, species with a high amount of axial parenchyma had faster production of callus tissue around the wound. The callus contains chemical compounds that act as barriers to prevent desiccation and protect tissue from pathogens (Haavik and Stephen, 2011). Arbellay et al. (2012) also affirm that the production of parenchyma around the wound, as a consequence of cambial injury, protects the living tissue.

It is not only axial parenchyma that has been shown to contribute to wound healing. In *Gallesia integrifolia* and *Guazuma ulmifolia*, the radial parenchyma also contributes to regeneration of cells; however, the height and width of the rays seems to be more relevant than ray frequency, as confirmed with *Alchornea glandulosa* which has uniseriate rays with high frequency, but with a low wound healing rate, as in *G. integrifolia* and *G. ulmifolia*. The composition of the rays is also important in xylem-phloem translocation. When the rays are composed by procumbent cells, translocation is more efficient (Carlquist, 1975), in turn improving wound healing.

The distribution of parenchyma tissue can be related to the pattern of wood healing. Specifically, the species that have axial parenchyma and produce a network between the vessels and rays through living tissue recover and provide passage of hormones that stimulate cell division of tissue near the wound. This, in turn, promotes the growth of callus tissue all around the wound area, accelerating wound closure. This phenomenon could be seen in *C. estrellensis*, *C. legalis*, *H. crysotrichus* and *I. sessilis*. On the other hand, the absence of axial parenchyma hinders such recovery by disabling affected regions, both above and below the injury, from producing sufficient wound healing tissue. In *G. integrifolia* and *G. ulmifolia*, callus tissue was formed only at the sides of the wound. In this case, the absence of the network between vessels and ray cells allows air to enter the xylem vessels through the wound, causing embolism by the Soil-Plant-Atmosphere Continuum (SPAC) pathway (McCulloh et al., 2004). Cavitation occurs more intensively above the wound, blocking hormone influx and redirecting these hormones to the wound sides. Below the wound, cytokinins will induce the regeneration of vessels and sieve tubes, as well as promote the production of callus from parenchyma cells around the wound (Aloni et al., 1990; Baum et al., 1991).

The production of parenchyma cells is related to hormonal activity. In particular, it is well known that gibberellin acts in synergism with auxin (Israelsson et al., 2005; Aloni, 2013). Gibberellin promotes cambial cell division (Dayan et al. 2012), while auxin promotes cell differentiation. However, in the absence of auxin, gibberellin will promote only cellular division (Wareing, 1958). Gibberellin has an important role in the induction of the wound healing process (Borchert et al., 1974). According to the intensity of the injury, it will transform mature tissue into juvenile tissue again (Taiz and Zeiger, 2006) and promote cellular division. In large concentrations, gibberellin will greatly enhance tissue growth (Bradley and Crane, 1957).

Apart from parenchyma, other anatomical characteristics related to wound healing rate are the intervessel pits and vessel ray pits. Pit size probably helps in the distribution of hormones to tissues around the wound, profiting by the increase in the process of cell division, as noted in *Ceiba speciosa*.

Fiber length which is controlled by gibberellin (Dayan et al., 2012) was also found to be related to wound healing rate as observed in *Ceiba speciosa*, *Cariniana estrellensis* and *C. legalis*, confirming the action of gibberellin on induction of wound healing. This relationship can also be observed in the interaction between proportion of parenchyma and fiber length founded in partial variation analyses. The presence of longer fibers is indicative of a larger amount of gibberellin (Dayan et al., 2012; Aloni,

2013). Aloni (2007) reported that increasing concentration of gibberellin produces fibers of greater length. Eriksson et al. (2000) even affirmed the existence of a specific gene that regulates the production of gibberellin so that the overexpression of this key regulatory gene results in improving the growth rate and biomass production with more numerous and longer xylem fibers. Therefore, by analyzing the phenotype related to fiber length, we can infer the genetic information of each species in relation to the amount of gibberellin produced in tissues. Asahina et al. (2002) showed that gibberellin production is involved in cell division during wound healing in the cortex of cucumber and tomato cut hypocotyls. Gibberellin is also utilized for wound healing in animals because it stimulates the activity and proliferation of fibroblasts, thus increasing collagen synthesis (Sharrif Moghaddasi and Kumar, 2011). This proves that cellular mechanisms that allow regeneration of tissues after damage might be shared by animals and plants (Reid and Ross, 2011).

## 5 CONCLUSIONS

Species longevity is related to their recovery ability against many kinds of injuries. This study showed the importance of axial and radial xylem parenchyma in wound healing, which is totally related to wound healing rate of species. The type and abundance of parenchyma tissue contribute to success in the wound healing process because it is responsible for supplying the production of new cells, maintaining vascular flow through transdifferentiation, and protecting against invasion of pathogenic organisms often responsible for wood decay. We can infer based on analyzing the phenotype related to fiber length that gibberellin has an important role in wound healing since it is a major signal responsible for stimulation of parenchyma proliferation after injury.

Based on the findings of this work we can conclude that the wood anatomy of tree functions as a fingerprint of metabolism and physiology, which can help a lot in understanding different mechanisms in tree life as in this case wound healing.

## 6 ACKNOWLEDGEMENTS

This study was financed, in part, by the Coordenação de Aperfeiçoamento de Pessoal de Nível Superior – Brazil (CAPES) – Finance-Code 001. The authors thank Sônia Regina Campião for laboratory support. Researcher Edenise Segala Alves (Instituto de Botânica) for manuscript contribution. Camila Moura Santos was supported by a research scholarship (145840/2012-3) from the Conselho Nacional de Desenvolvimento Científico e Tecnológico (CNPq).

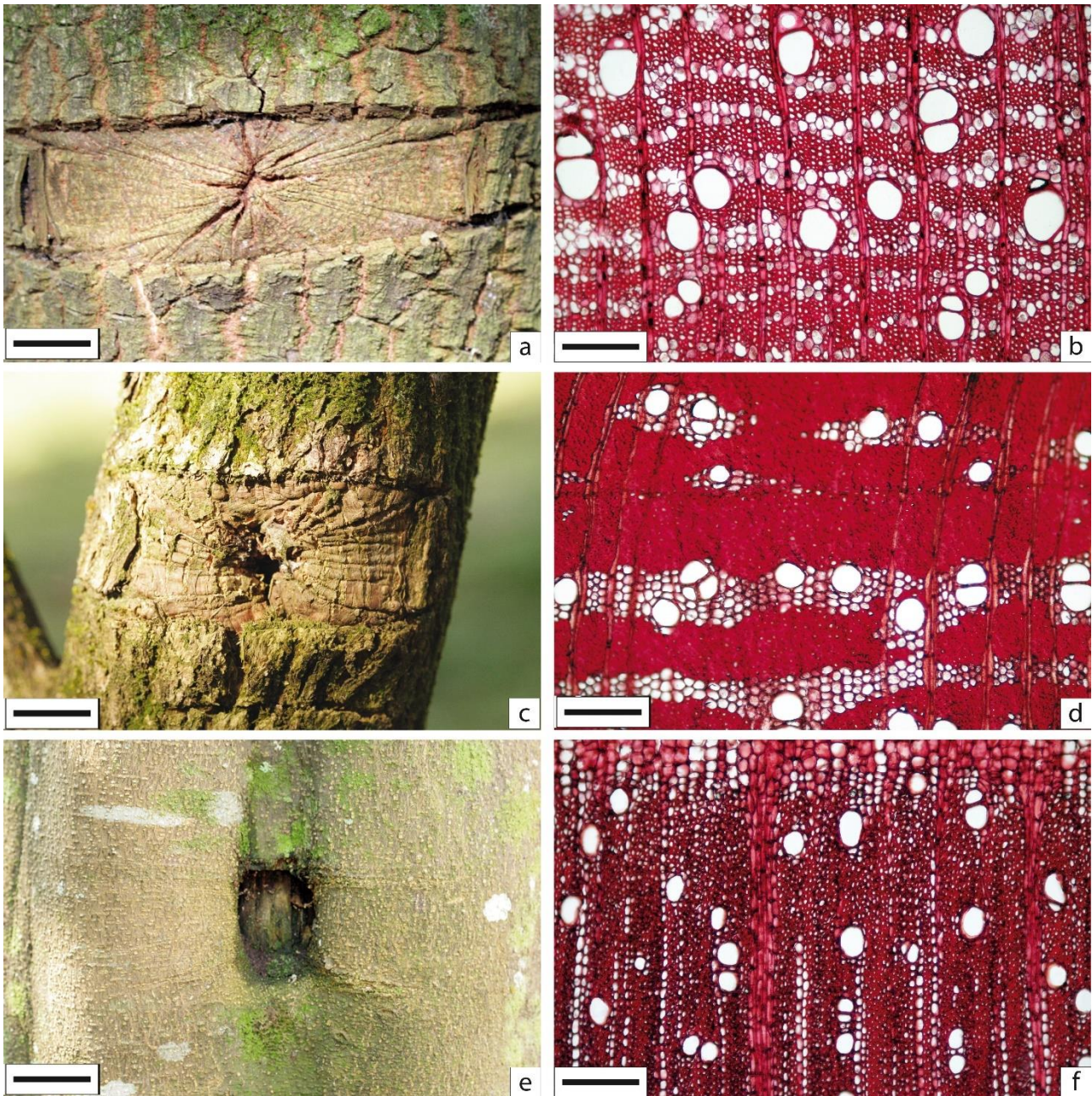


Figure 4. *Cariniana legalis* a, b; *Handroanthus chrysotrichus* c, d; *Gallesia integrifolia* e, f. Trunk healing after sample removal (left, scale bar = 2 cm). b. Transversal section (right, scale bar = 200 μm).

Figura 4. *Cariniana legalis* a, b; *Handroanthus chrysotrichus* c, d; *Gallesia integrifolia* e, f. Cicatrização do tronco após a remoção da amostra (esquerda, barra de escala = 2 cm). b. Seção transversal (direita, barra de escala = 200 μm).

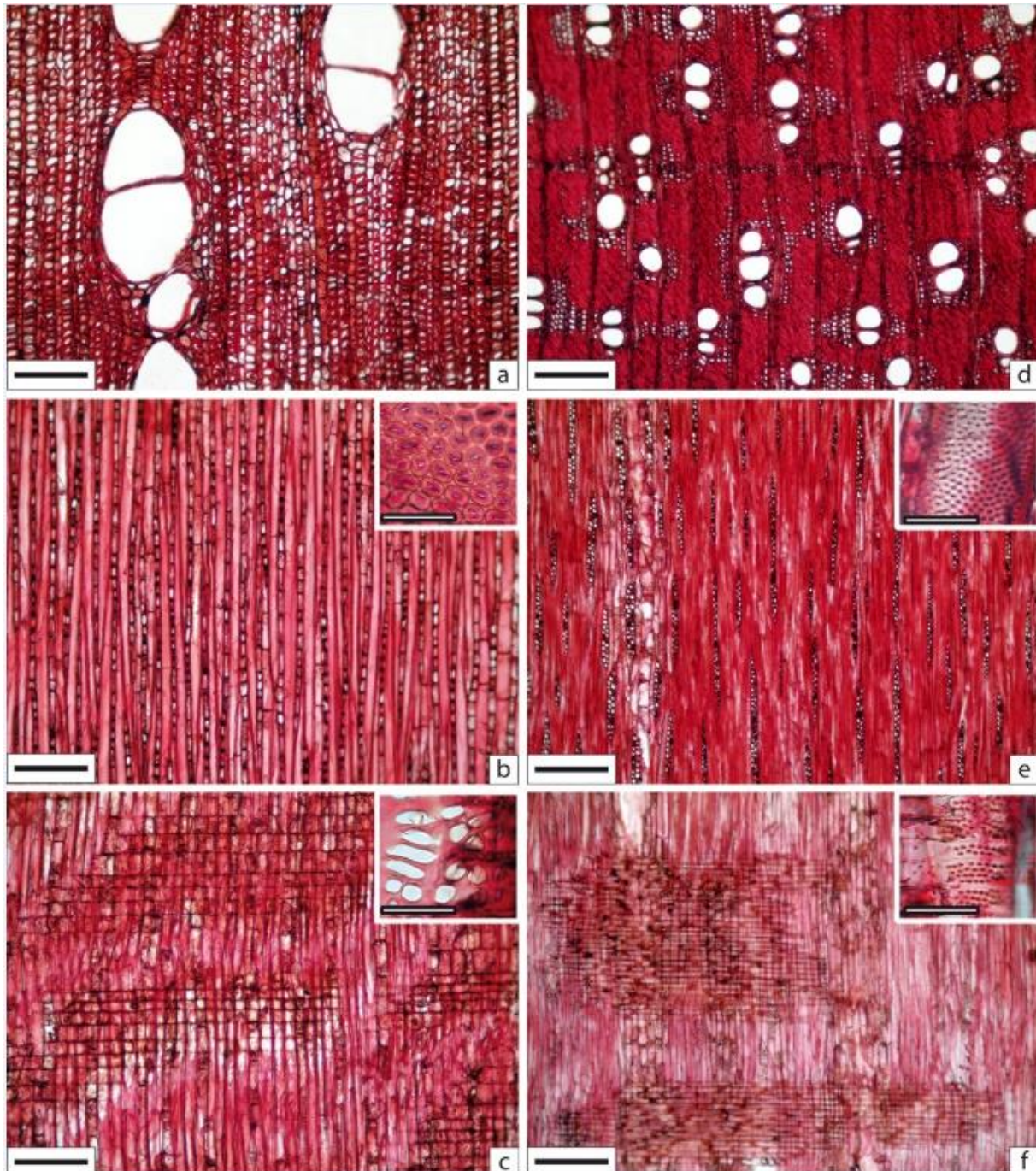


Figure 5. Wood sections of *Alchornea glandulosa* (a, b, c), *Paubrasilia echinata* (d, e, f), transversal sections (a, d) tangential sections with detail of the intervessel pits (b, e), radial sections with detail of vessel-ray pits (c, f) Bar = 200  $\mu$ m, detail bar = 50  $\mu$ m.

Figura 5. Seções do lenho de *Alchornea glandulosa* (a, b, c), *Paubrasilia echinata* (d, e, f), seções transversais (a, d) seções tangenciais com detalhe das pontoações intervasculares (b,e), seções radiais com detalhe das pontoações raiovasculares (c, f) Barra = 200  $\mu$ m, barra detalhe = 50  $\mu$ m.

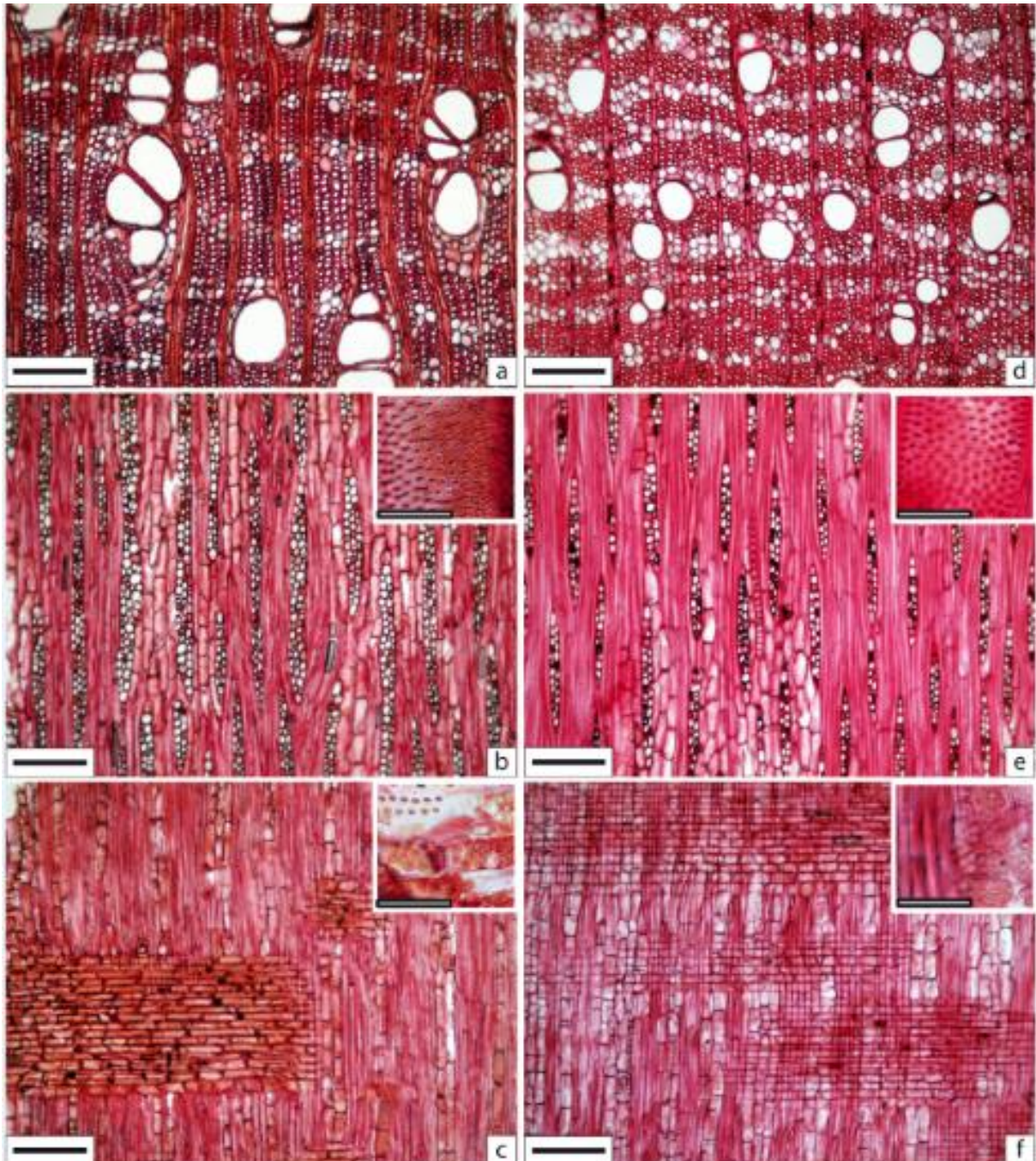


Figure 6. Wood sections of *Cariniana estrellensis* (a, b, c), *Cariniana legalis* (d, e, f), transversal sections (a, d) tangential sections with detail of the intervessel pits (b, e), radial sections with detail of the vessel-ray pits (c, f) Bar = 200 µm, detail bar = 50 µm.

Figura 6. Seções do lenho de *Cariniana estrellensis* (a, b, c), *Cariniana legalis* (d, e, f), seções transversais (a, d) seções tangenciais com detalhe das pontoações intervesselares (b, e), seções radiais com detalhe das pontoações raiovasculares (c, f) Barra = 200 µm, barra detalhe = 50 µm.

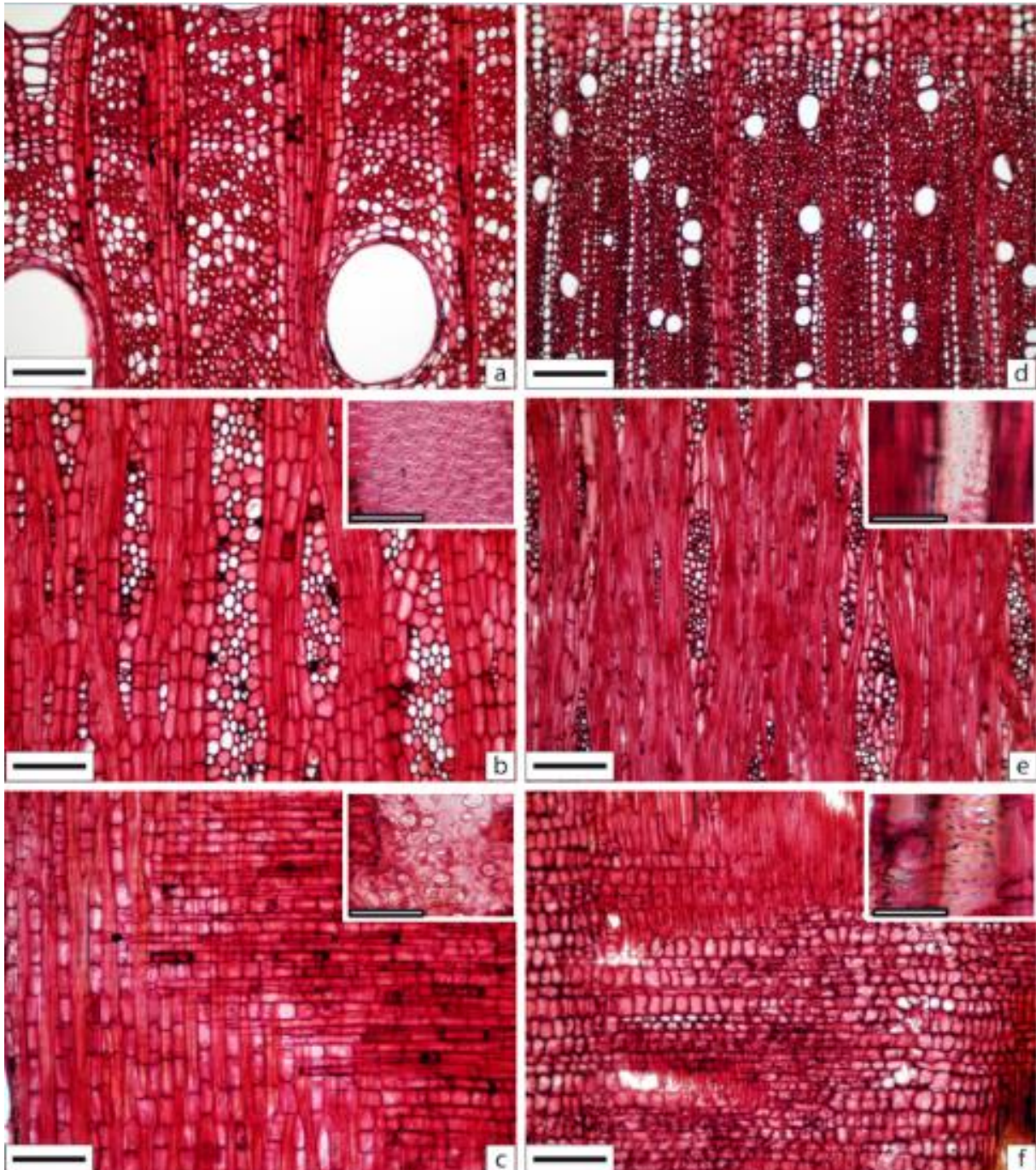


Figure 7. Wood sections of *Ceiba speciosa* (a, b, c), *Galesia integrifolia* (d, e, f), transverse sections (a, d) tangential sections with detail of the intervessel pits (b, e), radial sections with detail of the vessel-ray pits (c, f) Bar = 200 µm, detail bar = 50 µm.

Figura 7. Seções do lenho de *Ceiba speciosa* (a, b, c), *Galesia integrifolia* (d, e, f), seções transversais (a, d) seções tangenciais com detalhe das pontoações intervasculares (b, e), seções radiais com detalhe das pontoações raiovasculares (c, f) Barra = 200 µm, barra detalhe = 50 µm.

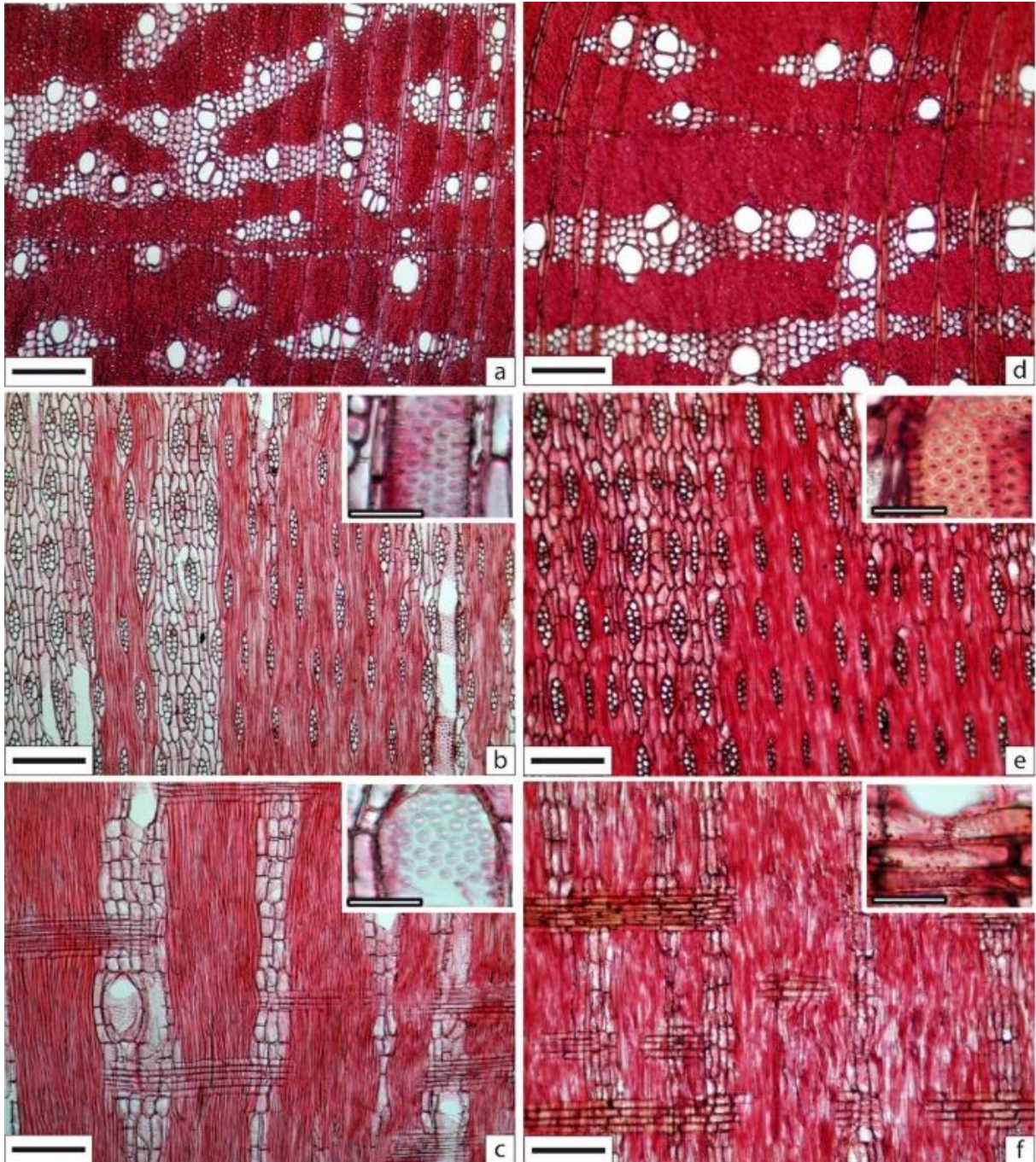


Figure 8. Wood sections of *Handroanthus heptaphyllus* (a, b, c), *Handroanthus chrysotrichus* (d, e, f), transversal sections (a, d) tangential sections with detail of the intervessel pits (b, e), radial sections with detail of the vessel-ray pits (c, f) Bar = 200  $\mu\text{m}$ , detail bar = 50  $\mu\text{m}$ .

Figura 8. Seções do lenho de *Handroanthus heptaphyllus* (a, b, c), *Handroanthus chrysotrichus* (d, e, f), seções transversais (a, d) seções tangenciais com detalhe das pontoações intervasculares (b, e), seções radiais com detalhe das pontoações raiovasculares (c, f) Barra = 200  $\mu\text{m}$ , barra detalhe = 50  $\mu\text{m}$ .

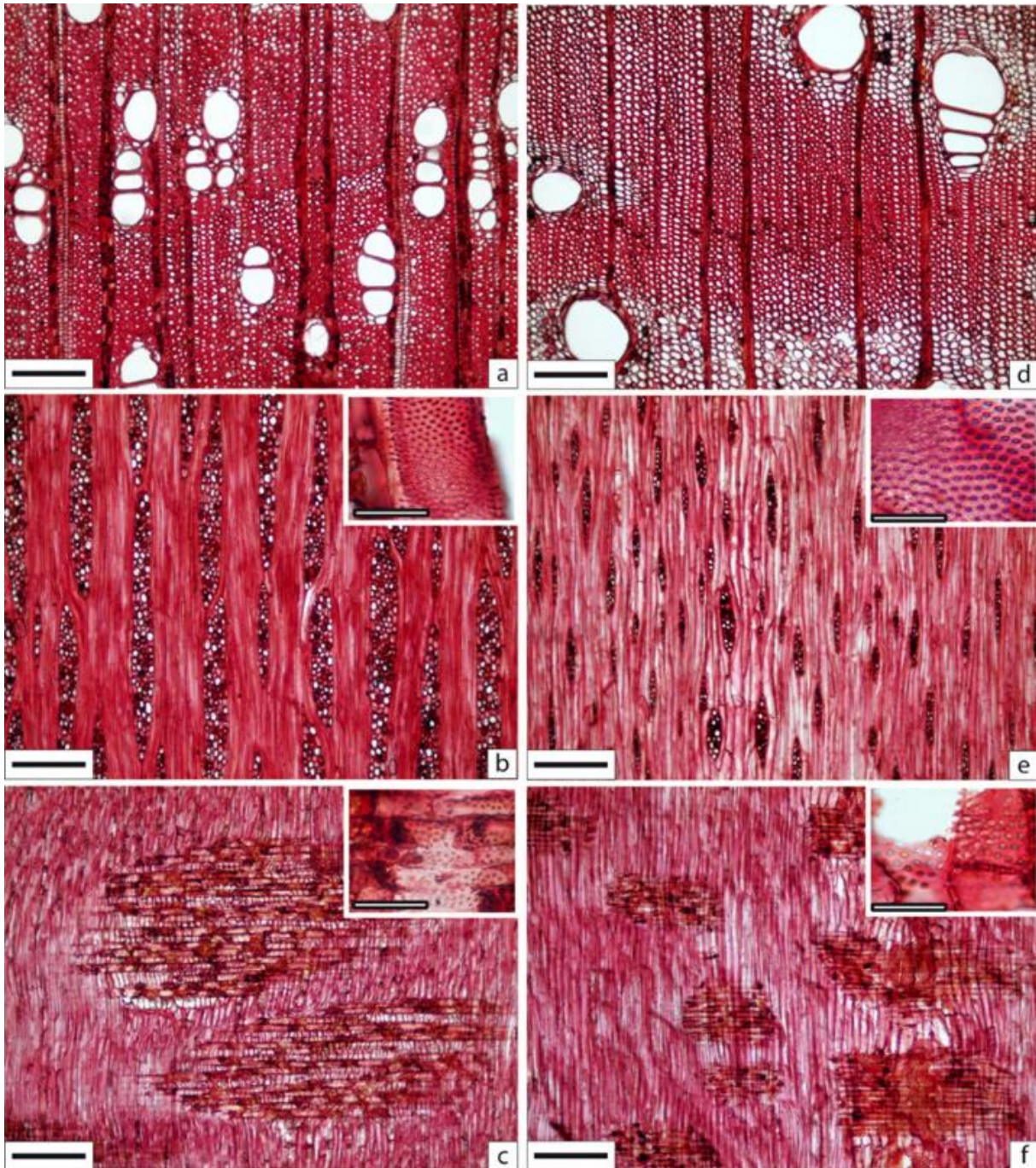


Figure 9. Wood sections of *Guazuma ulmifolia* (a, b, c), *Inga sessilis* (d, e, f), transversal sections (a, d) tangential sections with detail of the intervessel pits (b, e), radial sections with detail of the vessel-ray pits (c, f) Bar = 200  $\mu$ m, detail bar = 50  $\mu$ m.

Figura 9. Seções do lenho de *Guazuma ulmifolia* (a, b, c), *Inga sessilis* (d, e, f), seções transversais (a, d) seções tangenciais com detalhe das pontoações intervasculares (b, e), seções radiais com detalhe das pontoações raiovasculares (c, f) Barra = 200  $\mu$ m, barra detalhe = 50  $\mu$ m.

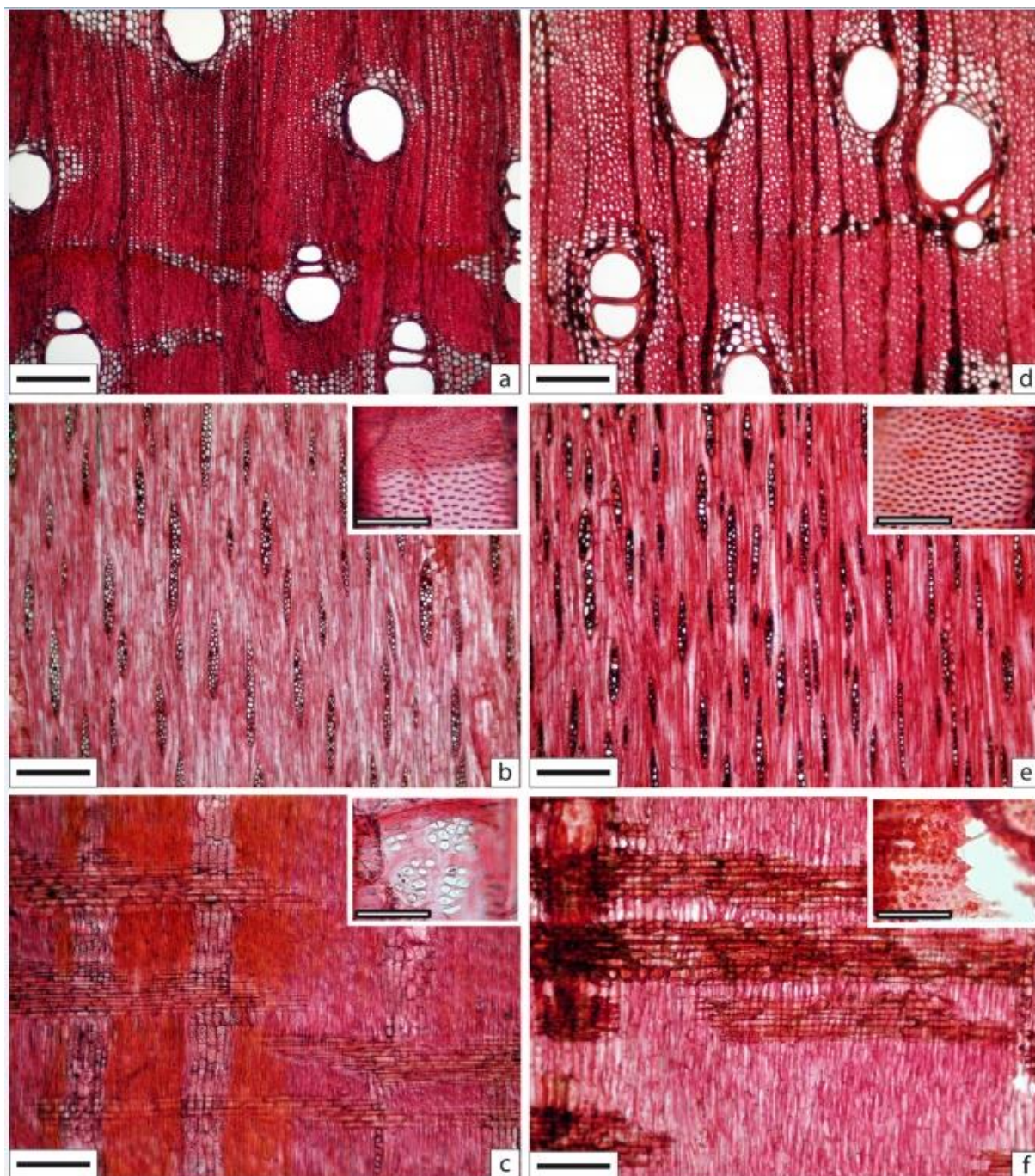


Figure 10. Wood sections of *Maclura tinctoria* (a, b, c), *Peltophorum dubium* (d, e, f), transversal sections (a, d) tangential sections with detail of the intervessel pits (b, e), radial sections with detail of vessel-ray pits (c, f) Bar = 200  $\mu$ m, detail bar = 50  $\mu$ m.

Figura 10. Seções do lenho de *Maclura tinctoria* (a, b, c), *Peltophorum dubium* (d, e, f), seções transversais (a, d) seções tangenciais com detalhe das pontoações intervasculares (b, e), seções radiais com detalhe das pontoações raiovasculares (c, f) Barra = 200  $\mu$ m, barra detalhe = 50  $\mu$ m.



Figure 11. Images of each individual trunk healing after 24 months of collection. The numbers identify the tree in the arboretum.

Figura 11. Imagens da cicatrização dos troncos de cada indivíduo após 24 meses da coleta. Os números identificam a árvore no arboreto.

## REFERENCES

- ALONI, R. Phytohormonal mechanisms that control wood quality formation in young and mature trees. In: ENTWISTLE, K.; HARRIS, P.; WALKER, J. (Eds.). **The compromised wood workshop**. New Zealand: The Wood Technology Research Centre, 2007. p. 1-22.
- ALONI, R. The induction of vascular tissues by auxin. In: DAVIES, P.J. (Ed.). **Plant hormones: biosynthesis, signal transduction, action!** Dordrecht: Kluwer Academic Publishers, 2010. p. 485-506.
- ALONI, R. The role of hormones in controlling vascular differentiation. In: FROMM, J. (Ed.). **Cellular Aspects of Wood Formation**. Berlin: Springer-Verlag, 2013. p. 99-139.
- ALONI, R.; BAUM, S.F.; PETERSON, C.A. The role of cytokinin in sieve tube regeneration and callose production in wounded *coleus* internodes. **Plant physiology**, v. 93, n. 3, p. 982-989, 1990.
- ARBELLAY, E.; FONTI, P.; STOFFEL, M. Duration and extension of anatomical changes in wood structure after cambial injury. **Journal of Experimental Botany**, v. 63, n. 8, p. 3271-3277, 2012.
- ASAHINA, M. et al. Gibberellin produced in the cotyledon is required for cell division during tissue reunion in the cortex of cut cucumber and tomato hypocotyls 1. **Plant physiology**, v. 129, n. 1, p. 201-210, 2002.
- BAUM, F.S.; ALONI, R.; PETERSON, C.A. Role of cytokinin in vessel regeneration in wound *Coleus* internodes. **Annals of Botany**, v. 67, n. 6, p. 543-548, 1991.
- BRADLEY, M.V.; CRANE, J.C. Gibberellin-stimulated cambial activity in stems of apricot spur shoots. **Science**, v. 126, n. 3280, p. 972-973, 1957.
- BORCHERT, R.; MCCHESENEY J.D.; WATSON, D. Wound healing in potato tuber tissue. **Plant physiology**, v. 53, n. 2, p. 187-191, 1974.
- BORCHERT, R.; POCKMAN, W.T. Water storage capacitance and xylem tension in isolated branches of temperate and tropical trees. **Tree physiology**, v. 25, n. 4, p. 457-466, 2005.
- BRODERSEN, C.R. et al. The dynamics of embolism repair in xylem: in vivo visualizations using high-resolution computed tomography. **Plant physiology**, v. 154, n. 3, p. 1088-1095, 2010.
- CARLQUIST, S. **Ecological strategies of xylem evolution**. Berkeley: University California Press, 1975. 259 p.
- CARLQUIST, S. **Comparative wood anatomy. Systematic, ecological, and evolutionary aspects of dicotyledon wood**, 2nd edn. Berlin: Springer - Verlag, 2001. 448 p.
- CHAPOTIN, S.M.; RAZANAMEHARIZAKA, J.H.; HOLBROOK, N.M. Baobab trees (*Adansonia*) in Madagascar use stored water to flush new leaves but not to support stomatal opening before the rainy season. **New phytologist**, v. 169, n. 3, p. 549-559, 2006.
- CHOAT, B.; JANSEN, S.; BRODRIBB, T.J., et al. Global convergence in the vulnerability of forests to drought. **Nature**, v. 491, n. 7426, p. 752-755, 2012.
- DAYAN, J. et al. Leaf-induced gibberellin signaling is essential for internode elongation, cambial activity, and fiber differentiation in tobacco stems. **The Plant Cell**, v. 24, n. 1, p. 66-79, 2012.
- ERIKSSON, M.E. et al. Increased gibberellin biosynthesis in transgenic trees promotes growth, biomass production and xylem fiber length. **Nature Biotechnology**, v. 18, n. 7, p. 784-788, 2000.
- EVERT, R.F. **Esau's Plant Anatomy: Meristems, cells, and tissues of the plant body: their structure, function, and development**. 3rd Edition, John Wiley and Son, New Jersey, 601 p.
- FISHER, J.B.; EWERS, F.W. Wound healing in stems of lianas after twisting and girdling injuries. **Botanical Gazette**, v. 150, n. 3, p. 251-265, 1989.
- FOX, J. The R Commander: A basic statistics graphical user interface to R. **Journal of Statistical Software**, v. 14, n. 9, p. 1-42, 2005.

ROMEIRO, D. et al. As anatomical features of the xylem could influence wound healing process in trees?

FUKUDA, H. Xylogenesis: initiation, progression, and cell death. **Annual review of plant physiology and plant molecular biology**, v. 47, p. 299-325, 1996.

GLASS, S.V.; ZELINKA, S.L. Moisture relations and physical properties of wood. In: ROSS R. (Ed.). **Wood handbook: wood as an engineering material**. Madison, U.S.A: Department of Agriculture, Forest Service, Forest Products Laboratory, 2010. p. 1-19.

HAAVIK, L.J.; STEPHEN, F.M. Factors that affect compartmentalization and wound closure of *Quercus rubra* infested with *Enaphalodes rufulus*. **Agricultural and Forest Entomology**, v. 13, n. 3, p. 291-300, 2011.

IAWA COMMITTEE. IAWA list of microscopic features for hardwood identification. **IAWA Bulletin**, v.10, p. 219-332, 1989.

IMASEKI, H. Hormonal Control of Wound-Induced Responses. In: PHARIS, R.P.; REID D.M. (Eds.) **Encyclopedia of plant physiology new series volume 11- hormonal regulation of development iii- role of environmental factors**. Berlin Heidelberg: Springer, 1985. p. 485-512.

ISRAELSSON, M.; SUNDBERG, B.; MORITZ, T. Tissue-specific localization of gibberellins and expression of gibberellin-biosynthetic and signaling genes in wood-forming tissues in aspen. **The Plant journal: for cell and molecular biology**, v. 44, n. 3, p. 494-504, 2005.

KRAUS, J.E.; ARDUIN, M. **Manual básico de métodos em morfologia vegetal**. Rio de Janeiro: Editora EDUR, 1997. 198 p.

LARJAVAARA, M.; MULLER-LANDAU, H.C. PERSPECTIVE: Rethinking the value of high wood density. **Functional Ecology**, v. 24, n. 4, p. 701-705, 2010.

LIGGES, U.; MÄCHLER, M. Scatterplot3d - an R Package for visualizing multivariate data. **Journal of Statistical Software**, v. 8, n. 11, p. 1-20, 2003.

MCCULLOH, K.A.; SPERRY, J.S.; ADLER, F.R. Murray's law and the hydraulic vs mechanical functioning of wood. **Functional ecology**, v. 18, n. 2, p. 931-938, 2004.

MORRIS, H. et al. The parenchyma of secondary xylem and its critical role in tree defense against fungal decay in relation to the CODIT model. **Frontier in Plant Science**. 7:1665. doi: 10.3389/fpls.2016.01665

NEELY, D. Tree wound closure. **Journal of Arboriculture**, v. 14, n. 6, p. 148-152, 1988.

OKSANEN, J. et al. vegan: Community Ecology Package. R package version 2.3-0. Available at: <<http://CRAN.R-project.org/package=vegan>>. Access on: 17 apr. 2015.

OSTRY, M.E.; VENETTE, R.C.; JUZWIK, J. Decline as a disease category: is it helpful? **Phytopathology**, v. 101, n. 4, p. 404-409, 2011.

PANG, Y. et al. Phloem transdifferentiation from immature xylem cells during bark regeneration after girdling in *Eucommia ulmoides* Oliv. **Journal of experimental botany**, v. 59, n. 6, p. 1341-1351, 2008.

R CORE TEAM. R: A language and environment for statistical computing. R Foundation for Statistical Computing, Vienna, Austria. Available at: <<http://www.R-project.org/>>. Access on: 02 may. 2015.

REID, J.B.; ROSS, J.J. Regulation of tissue repair in plants. **Proceedings of the National Academy of Sciences of the United States of America**, v. 108, n. 42, p. 17241-17242, 2011.

SCHMITT, U.; LIESE, W. Wound reaction of the parenchyma in *Betula*. **IAWA Bulletin**, v. 11, n. 4, p. 413-420, 1990.

SCHMITT, U.; LIESE, W. Wound tyloses in *Robinia pseudoacacia* L. **IAWA Journal**, v. 15, n. 2, p. 157-160, 1994.

SCHWARZE, F.W.M.R. Wood decay under the microscope. **Fungal Biology Reviews**, v. 21, n. 4, p. 133-170, 2007.

SHARRIF MOGHADDASI, M.; KUMAR, S.V. *Aloe vera* their chemicals composition and applications: A review. **International Journal of Biological & Medical Research**, v. 2, n. 1, p. 466-471, 2011.

ROMEIRO, D. et al. As anatomical features of the xylem could influence wound healing process in trees?

STOBBE, H. et al. Developmental stages and fine structure of surface callus formed after debarking of living lime trees (*Tilia* sp.). **Annals of Botany**, v. 89, n. 6, p. 773-782, 2002.

TAIZ, L.; ZEIGER, E. **Plant Physiology**, Fourth Edition. Sunderland: Sinauer Associates, 2006. 764 p.

TOLEDO, J.J.; MAGNUSSON, W.E.; CASTILHO, C.V. Competition, exogenous disturbances and senescence shape tree size distribution in tropical forest: evidence from tree mode of death in Central Amazonia. **Journal of Vegetation Science**, v. 24, n. 4, p. 651-663, 2013.

TYREE, M.T. et al. Refilling of embolized vessels in young stems of laurel. Do we need a new paradigm? **Plant physiology**, v. 120, n. 1, p. 11-22, 1999.

UGGLA, C. et al. Function and dynamics of auxin and carbohydrates during earlywood/latewood transition in scots pine. **Plant physiology**, v. 125, n. 4, p. 2029-2039, 2001.

YADETA, K.A.; THOMMA, B.P.H.J. The xylem as battleground for plant hosts and vascular wilt pathogens. **Frontiers in plant science**, v. 4, n. 97, p. 1-12, 2013.

WAREING, F.B. Interaction between indole-acetic acid and gibberellic acid in cambial activity. **Nature**, v. 181, p. 1744-1745. 1958.

ZWIENIECKI, M.A.; HOLBROOK, N.M. Confronting Maxwell's demon: biophysics of xylem embolism repair. **Trends in plant science**, v. 14, n. 10, p. 530-534, 2009.